Acknowledgments: This work has been realised with the financial support of the CICYT (TIC 2002-04569-C02-01) and CICYT (TIC 2001-3839-C03-01/02/03). The authors also wish to thank Texas Instruments for the donation of equipment through an Elite Project.

3 March 2003
Electronics Letters Online No: 20030566
DOI: 10.1049/el:20030566

J.M. Pardo and J.L. Jimenez (*Department of Audiovisual Engineering and Communications, Polytechnical University of Madrid, Ctra. Valencia Km. 7, Madrid 28031, Spain*)

E-mail: impardo@gmr.ssr.upm.es

M. Burgos (*Department of Signals, Systems and Radiocommunications, Polytechnical University of Madrid, Ciudad Universitaria S/N, Madrid 28040, Spain*)

References

1 GARDNER, W.A.: 'Exploitation of spectral redundancy in cyclostationary signals', *IEEE Signal Process Mag.*, 1991, pp. 14–36
2 GARDNER, W.A., and SPOONER CHAD, M.: 'Signal interception: performance advantages of cyclic-feature detectors', *IEEE Trans. Commun. Technol.*, 1992, **40**, pp. 149–159
3 1st Int. Workshop on Noise Radar Technology NRTW'2002, Yalta, Ukraine, 2002

Autocorrelation functions for Hermite-polynomial ultra-wideband pulses

L.E. Miller

Communication systems using carrierless ultra-wideband (UWB) pulse waveforms are being considered for high-rate wireless networks. The autocorrelation functions are given for models of UWB pulses based on Hermite polynomials, for use in predicting system performance.

Introduction: Multiple-access communications using carrierless ultra-wideband (UWB) pulses have been proposed for fading environments [1] and for high-rate indoor networks [2]. Transmitter and receiver antennas may differentiate such pulses, resulting in waveforms resembling very short sinusoidal bursts. Pulses based on Hermite polynomials, which are generated by successive differentiation of a 'Gaussian-shaped' pulse, have been proposed as mathematical models for UWB pulses because of their resemblance to actual waveforms [3, 4]. While many properties of Hermite polynomials are well established for various applications, their autocorrelation properties as time functions have not been published previously. In this Letter, the autocorrelation functions for Hermite-polynomial pulses are shown, including an iterative relation for generating them.

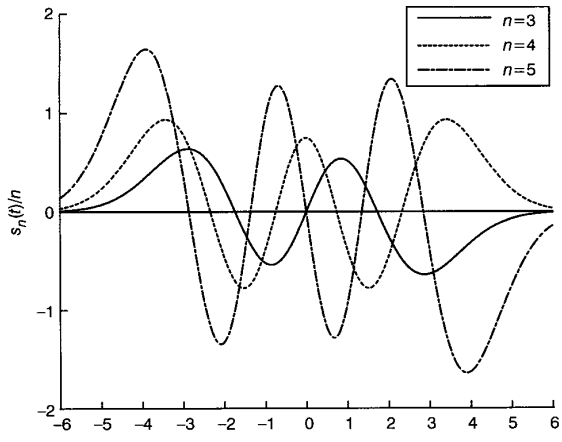

Fig. 1 *Example UWB waveforms based on Hermite polynomials*

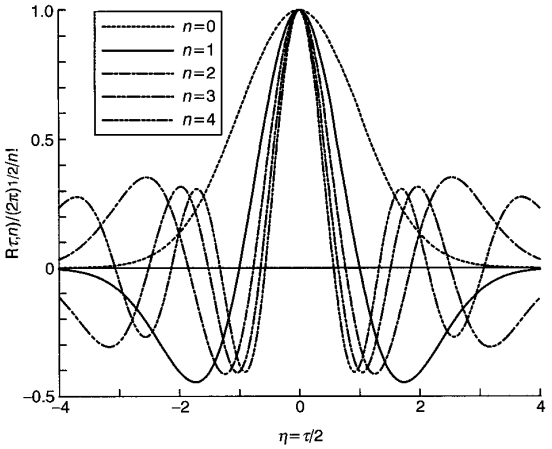

Fig. 2 *Example autocorrelation functions for UWB waveforms based on Hermite polynomials*

Model: A model pulse shape for UWB communications is [4]

$$s_n(t) = e^{-t^2/4} \quad He_n(t) = e^{t^2/4}(-1)^n \frac{d^n}{dt^n}(e^{-t^2/2}) \tag{1}$$

where $He_n(t)$ is the nth degree Hermite polynomial [5], which has n zero crossings. The Hermite polynomials may be generated using the iteration [5]

$$\begin{aligned} He_{n+1}(x) &= xHe_n(x) - nHe_{n-1}(x), \\ He_0(x) &= 1, \quad He_1(x) = x \end{aligned} \tag{2}$$

Examples of this family of pulse shapes are given in Fig. 1.

Derivation of autocorrelation function: Using $\eta = \tau/2$ for notational convenience, the autocorrelation function for the pulse waveform of (1) is given by

$$R(\tau; n) = \int_{-\infty}^{\infty} s_n(t)s_n(t-\tau)dt = \int_{-\infty}^{\infty} s_n(t+\eta)s_n(t-\eta)dt \tag{3}$$

Substituting (1) leads to the expression

$$R(\tau; n) = \sqrt{2\pi}e^{-\eta^2/2}E_t\{He_n(t+\eta)He_n(t-\eta)\} \tag{4}$$

where $E_t\{\}$ denotes expectation as if t were a zero-mean, unit-variance Gaussian random variable. For example, by direct calculation we find that

$$\begin{aligned} R(\tau; 0) &= \sqrt{2\pi}e^{-\eta^2/2}E_t\{1\} = \sqrt{2\pi}e^{-\eta^2/2} \\ R(\tau; 1) &= \sqrt{2\pi}e^{-\eta^2/2}E_t\{t^2 - \eta^2\} = \sqrt{2\pi}e^{-\eta^2/2}(1-\eta^2) \\ R(\tau; 2) &= \sqrt{2\pi}e^{-\eta^2/2}E_t\{t^4 - 2t^2(\eta^2+1) + \eta^4 - 2\eta^2 + 1\} \\ &= \sqrt{2\pi}e^{-\eta^2/2}(2 - 4\eta^2 + \eta^4) \\ R(\tau; 3) &= \sqrt{2\pi}e^{-\eta^2/2}E_t\{t^6 - 3t^4(\eta^2+2) + 3t^2(\eta^4+3) \\ &\quad - \eta^6 + 6\eta^4 - 9\eta^2\} \\ &= \sqrt{2\pi}e^{-\eta^2/2}(6 - 18\eta^2 + 9\eta^4 - \eta^6) \\ R(\tau; 4) &= \sqrt{2\pi}e^{-\eta^2/2}E_t\{t^8 - 4t^6(\eta^2+3) \\ &\quad + 6t^4(\eta^4 + 2\eta^2 + 7) - 4t^2(\eta^6 - 3\eta^4 + 9\eta^2 + 9) \\ &\quad + \eta^8 - 12\eta^6 + 42\eta^4 - 36\eta^2 + 9\} \\ &= \sqrt{2\pi}e^{-\eta^2/2}(24 - 96\eta^2 + 72\eta^4 - 16\eta^6 + \eta^8) \end{aligned} \tag{5}$$

The general form corresponding to (5) is somewhat subtle but is found by inspection to be

$$R(\tau; n) = \sqrt{2\pi}e^{-\eta^2/2}\sum_{k=0}^{n}\frac{n!}{k!}\binom{n}{k}(-1)^k\eta^{2k} \tag{6}$$

An iterative relation is desirable for computation. To derive an iterative relation, we note that (6) can be expressed in terms of a confluent hypergeometric function, as follows:

$$R(\tau; n) = \sqrt{2\pi}e^{-\eta^2/2}n! \sum_{k=0}^{\infty} \frac{\eta^{2k}}{k!} \frac{(-n)_k}{(1)_k}$$
$$= \sqrt{2\pi}e^{-\eta^2/2}n!\,{}_1F_1(-n; 1; \eta^2) \quad (7)$$

where $(a)_k = \Gamma(a+k)/\Gamma(a)$ is Pochammer's symbol. We may use Kummer's transformation [6] to write

$${}_1F_1(-n; 1; \eta^2) = e^{\eta^2}\,{}_1F_1(n+1; 1; -\eta^2) \quad (8)$$

in order to apply a recursion formula for the hypergeometric function [6, formula 13.4.1] to obtain

$$(n+1)\,{}_1F_1(n+2; 1; -\eta^2) = (2n+1-\eta^2)\,{}_1F_1(n+1; 1; -\eta^2) - n\,{}_1F_1(n; 1; -\eta^2) \quad (9)$$

Applying this recursion to the autocorrelation function in (7), we have the following recursion:

$$R(\tau; n+1) = (2n+1-\eta^2)R(\tau; n) - n^2R(\tau; n-1) \quad (10)$$

with η, $R(\tau; 0)$, and $R(\tau; 1)$ as given above, e.g.

$$R(\tau; 4) = (7-\eta^2)R(\tau; 3) - 9R(\tau; 2) \quad (11)$$

which yields the results for $R(\tau; 4)$ that is shown above. Example plots of the autocorrelation function for the UWB pulses based on Hermite polynomials are shown in Fig. 2 after normalisation by the maximum value.

2 April 2003
Electronics Letters Online No: 20030550
DOI: 10.1049/el:20030550

L. E. Miller (*National Institute of Standards and Technology, Gaithersburg, Maryland, USA*)

E-mail: lmiller@antd.nist.gov

Reference

1 RAMIREZ-MIRELES, F.: 'On the performance of ultra-wideband signals in Gaussian noise and dense multipath', *IEEE Trans. Veh. Technol.*, 2001, **50**, pp. 244–249
2 WITHINGTON, P.: 'Ultra-wideband RF—a tutorial', IEEE 802.15 Working Group on Wireless Personal Area Networks (WPANs), document 802.15-00/083r0, March 2000 (Available online at http://grouper.ieee.org/groups/802/15/pub/2000/Mar00/)
3 CORRAL, C., *et al.*: 'Pulse spectrum optimization for ultra-wideband communication'. Proc. 2002 IEEE Conf. on Ultra Wideband Systems and Technologies, Baltimore, MA, USA, May 2002
4 MICHAEL, L.B., GHAVAMI, M., and KOHNO, R.: 'Multiple pulse generator for ultra-wideband communication using Hermite polynomial based orthogonal pulses'. Proc. 2002 IEEE Conf. on Ultra Wideband Systems and Technologies, Baltimore, MA, USA, May 2002
5 HOCHSTRASSER, U.W.: 'Orthogonal polynomials' Chap. 22 of ABRAMOWITZ, M., and STEGUN, A. (Eds.): 'Handbook of mathematical functions', National Bureau of Standards (now NIST) Applied Mathematics Series 55, Government Printing Office, Washington, 1970
6 SLATER, L.J.: 'Confluent hypergeometric functions' Chap. 13 of ABRAMOWITZ, M., and STEGUN, A. (Eds.): 'Handbook of mathematical functions', National Bureau of Standards (now NIST) Applied Mathematics Series 55, Government Printing Office, Washington, 1970

Downlink radio resource allocation for multibeam satellite communications

Kwangjae Lim and Sooyoung Kim

To increase system capacity and allow downlink beams to share orthogonal radio resources, a synchronous transmission for downlink signals in a multibeam satellite communication system is proposed. Also presented is an optimum radio resource allocation for packet transmission in the synchronous multibeam system.

Introduction: In typical satellite-based CDMA cellular systems [1, 2], full frequency reuse is applied for high spectral efficiency, as in terrestrial CDMA cellular systems. Different scrambling codes, such as pseudo noise (PN) sequences, are used for discriminating each signal for downlink beams. In such conventional satellite systems, the adjacent beams generate a serious interbeam interference to the desired beam because of the non-orthogonality between the PN scrambling codes and the imperfect isolation of the satellite antenna radiation pattern. We refer to this conventional system as the *asynchronous* system in this Letter. However, all the downlink signals can be synchronised on both the transmission and reception sides because the satellite is the only signal source. This is the basic idea of the *synchronous* system proposed in this Letter. In the synchronous multibeam satellite system, the limited radio resources should be carefully used and, thus, an efficient radio resource allocation is required for co-ordinated resource usage. This Letter proposes a synchronous multibeam satellite system and a dynamic radio resource allocation for the packet transmission.

Synchronous multibeam satellite system: We consider a multibeam satellite system where the mobile packet services are provided to users by a fixed earth station (FES) through a geosynchronous-orbit (GSO) satellite. The downlink radio resource is divided into multiple radio resource units (RRUs) by time, frequency, and code division multiplexing. Each RRU is defined by a specific spreading code in a specific frequency/time slot. All downlink signals are synchronised in both the time and frequency domains. Due to the synchronised transmission, all beams can share the orthogonal radio resources. In principle, this eliminates the interbeam interference due to the orthogonality between RRUs. However, in mobile environments, the orthogonality between different spreading codes in the same frequency/time slot can be broken by time-dispersive multipath (frequency-selective) fading. In this Letter, we consider the imperfect RRU orthogonality as an interference factor between orthogonal spreading codes. Under heavy load conditions, the number of available RRUs in a beam may be restricted since all beams share a common RRU set. To avoid this resource limitation, RRUs are reused in different beams if the interbeam interference can be ignored due to a sufficient isolation of radiation patterns between the different beams. The radio resource allocation proposed in this Letter controls the interbeam interference by properly allocating and reusing the orthogonal RRUs.

Received SIR model: The received SIR of a packet, which is transmitted from beam b to user u in an RRU (s, l, m) defined by frequency slot s, time slot l, and spreading code m, is modelled by,

$$\gamma_{b,u(s,l,m)} = SF\frac{p_{b,(s,l,m)}g_{b,u}}{I_{b,u,(s,l)} + Z_{b,u,(s,l)} + N_{noise}} \quad (1)$$

where SF, $p_{b,(s,l,m)}$, $g_{b,u}$, $I_{b,u,(s,l)}$, $Z_{b,u,(s,l)}$, and N_{noise} represent the spreading gain, the transmit power used in RRU (s, l, m), the link gain between user u and beam b, the intrabeam interference and the interbeam interference in frequency/time slot (s, l), and background noise power, respectively. The interferences in (1) are expressed by,

$$I_{b,u,(s,l)} = \kappa_1 \sum_{\substack{i \in V_{b,(s,l)},\\ i \neq m}} p_{b,(s,l,i)}g_{b,u} \quad (2)$$

$$Z_{b,u,(s,l)} = \kappa_2 \sum_{\substack{j \in B,\\ j \neq b}} \sum_{i \in V_{j,(s,l)},} p_{j,(s,l,i)}g_{j,u} + \kappa_3 \sum_{\substack{j \in B,\\ j \neq b}} p_{j,(s,l,m)}g_{j,u} \quad (3)$$

where B, $V_{b,(s,l)}$, and κ_x $(x = 1, 2, 3)$ are the set of beams, the set of RRUs in frequency/time slot (s, l) of beam b, and the interference factors, respectively. The interference factors are set by $\kappa_1 = \kappa_2 = \kappa$ and $\kappa_3 = SF$ for the synchronous system, and $\kappa_1 = \kappa$ and $\kappa_2 = \kappa_3 = 1$ for the asynchronous system, where κ stands for the interference factor between different orthogonal codes due to frequency-selective fading.

Radio resource allocation: Every user in the service measures the received power of the service and adjacent beam pilots and periodically reports them to a resource control centre, which is located at either the FES or satellite. The centre estimates the link gains on downlink beams from the user report and allocates RRUs and transmit power using the estimated link gains. For each packet transmission,